

S100A8/S100A9 and their association with cartilage and bone

H. Zreiqat · C. R. Howlett · S. Gronthos ·
D. Hume · C. L. Geczy

Received: 11 June 2007 / Accepted: 20 June 2007 / Published online: 17 July 2007
© Springer Science+Business Media B.V. 2007

Abstract S100A8 and S100A9 are calcium-binding proteins expressed in myeloid cells and are markers of numerous inflammatory diseases in humans. S100A9 has been associated with dystrophic calcification in human atherosclerosis. Here we demonstrate S100A8 and S100A9 expression in murine and human bone and cartilage cells. Only S100A8 was seen in preosteogenic cells whereas osteoblasts had variable, but generally weak expression of both proteins. In keeping with their reported high-mRNA expression, S100A8 and S100A9 were prominent in osteoclasts. S100A8 was expressed in alkaline phosphatase-positive hypertrophic chondrocytes, but not in proliferating chondrocytes within the growth plate where the cartilaginous matrix was calcifying. S100A9 was only evident in the invading vascular osteogenic tissue penetrating the degenerating chondrocytic zone adjacent to the primary spongiosa, where S100A8 was also expressed. Whilst, S100A8 has been shown to be associated with osteoblast differentiation, both S100A8 and S100A9 may contribute

to calcification of the cartilage matrix and its replacement with trabecular bone, and to regulation of redox in bone resorption.

Keywords S100A8 · S100A9 · Osteoblasts · Chondrocytes · Osteoclasts · Cartilage

Introduction

S100 proteins belong to the superfamily of calcium-binding proteins that regulate key cellular pathways, many involving calcium as a second messenger. They are recently evolved and structurally related to calmodulin (Ravasi et al. 2004). Human S100s include 21 highly conserved members, 17 of which are located within the 1q21.3 gene cluster. S100 protein expression has strong associations with human disease (McNutt et al. 1998; Donato et al. 2001). Intracellular functions include regulation of growth, apoptosis (Makino et al. 2004), suppression of tumor progression (Al-Rasheed et al. 2003; Helfman et al. 2005), regulation of intracellular redox (Kerkhoff et al. 2005) and embryogenesis (Passey et al. 1999a, b). Some have extracellular, cytokine-like activities involving regulation of the cytoskeleton (Vogl et al. 2004), effects on cell migration (Cornish et al. 1996) and adhesion, and in host and oxidative defence (Engelkamp et al. 1993; Raftery et al. 2001; Yang et al. 2001; Harrison et al. 1999). The receptor for advanced glycosylation end products (RAGE) is a putative S100 receptor (Hofmann et al. 1999), although additional receptors, as yet uncharacterized, are proposed (Sorci et al. 2003, 2004).

The myeloid-associated “calgranulins” S100A8 (A8, MRP-8) and S100A9 (A9, MRP14) are abundant constitutive cytoplasmic proteins in neutrophils and to a lesser

H. Zreiqat (✉)
Biomaterials and Tissue Engineering Research Unit, Biomedical Engineering, School of AMME, The University of Sydney, Sydney, NSW 2006, Australia
e-mail: hzreiqat@usyd.edu.au

C. R. Howlett · C. L. Geczy
Inflammatory Diseases Research Unit, School of Medical Sciences, University of NSW, Sydney, NSW 2052, Australia

S. Gronthos
Mesenchymal Stem Cell Group, Institute of Medical and Veterinary Science/Hanson Institute, Adelaide, SA 2005, Australia

D. Hume
Institute for Molecular Bioscience, University of Queensland, Queensland, QLD 4072, Australia

extent, in monocytes (reviewed in Roth et al. 2003). The expression of the two genes is a marker for the onset of myelopoiesis in the liver of the developing mouse. Although both genes are commonly expressed together, A8 alone is expressed in the ectoplacental cone shortly after implantation and, in keeping with a function for A8 at this location, mutation in the A8 gene is embryonic lethal due to failure of implantation (Hobbs et al. 2003; Passey et al. 1999a, b). In contrast, mice with a null mutation in A9 are born with expected Mendelian frequency, and are viable and fertile. Neutrophils from A9 null mice also lack A8 protein (but not mRNA), yet despite the loss of two of the most abundant proteins in the cell, only marginal changes in function were described and there is no apparent compensatory expression of other calcium-binding proteins (Hobbs et al. 2003; Manitz et al. 2003). A8 and A9 can form a hetero-complex known as calprotectin that is a clinical laboratory marker of inflammation (Foell et al. 2004; McNutt 1998).

Given the apparent redundancy of A8 and A9 in myeloid cells, we were interested in exploring other sites of expression where the function might be indispensable. The presence of S100 proteins in cartilage and bone was reported previously (Balmain et al. 2003; Duarte et al. 2003) but the specificities of the antibodies used (to S100A1/B) are unclear and their cross-reactivity with other S100 proteins undefined. More recently, another S100 family member, S100A4, also expressed in myeloid cells (Ravasi et al. 2004), was found in differentiating osteoblasts and was shown to diminish bone matrix mineralization (Duarte et al. 2003). S100A2 was detected in chondrocytes within calcifying areas of epiphyseal cartilage suggesting its involvement in cartilage calcification (Balmain et al. 2003). Here we explore the expression of A8 and A9 in mouse and human cartilage and bone using immunohistochemistry with specific antibodies, and found them in key cells involved in bone turnover. The two proteins were expressed at high levels in cartilage and bone, but in distinct locations, and could contribute to regulation of cartilage and bone development.

Materials and methods

Mice and human samples

Experimentation was in compliance with guidelines from the National Health & Medical Research Council of Australia and the New South Wales University Animal Care and Ethics Committee (No 00/66). Outbred CD1 mice maintained under specific pathogen-free conditions and fed normal chow ad libitum, were used at 2, 4, and 8 weeks old. Permission to use discarded human tissue was granted

by the Human Ethics Committee of the University of New South Wales (No. 97043). A small amount of cartilagenous tissue was available from a 2-year-old boy undergoing corrective surgery.

Tissue preparation

Samples were fixed immediately after sacrifice in either 4% w/v paraformaldehyde or cold 95% alcohol for paraffin or resin embedding, respectively. After fixation, tissue for paraffin embedding was decalcified at 4°C in 15% ethylenediaminetetra-acetic acid di-sodium salt (EDTA)/0.5% paraformaldehyde/phosphate-buffered saline (PBS) at pH 8.0, while slowly rotated; decalcifying solution was changed daily over 7 days. Decalcified samples were dehydrated in ascending solutions of ethanol and embedded in paraffin.

Resin (hydroxyethylmethacrylate)-embedded and fixed tissues were treated with an intermediate infiltrating solution, 95% Histo-resin (Leica kit, Heidelberg, BRD, Germany), followed by total infiltration through two changes of cold 100% Histo-resin as described (Laboux 2003). Tissue was then embedded in HistoMold and polymerization completed at room temperature.

Paraffin and resin sections (4 µm) were cut with a microtome (Leitz 121, Baden-Wurttemberg, Germany) or a heavy-duty microtome (Reichert-Jung, Leica, Germany), respectively, collected on chrome alum-gelatin-coated glass slides and air-dried at room temperature.

Immunohistochemistry

Immunostaining was carried out with rabbit polyclonal IgG purified on Protein A-Sepharose and raised against mouse or human recombinant A8 and A9 as described (Iismaa et al. 1994). The antibodies (Abs) to A8 did not cross-react with A9 and vice versa; the Abs did not cross-react with human S100A12, S100B or S100A1. Controls included replacement of primary Abs with Hanks balanced salt solution (HBSS; Life Technologies, Gaithersburg, MD, USA) and non-immune rabbit IgG used at the same concentration.

De-paraffinized and resin-embedded etched sections (incubated in acetone for 20 min) were blocked with 2% bovine serum albumin (BSA) in HBSS for 1 h before primary Abs were applied at the appropriate concentrations (pre-determined by serial dilution), and sections were incubated overnight in a humidified chamber at 4°C. Sections were then washed three times with Tris-buffered saline 1 (TBS1, 0.1 M Tris HCl, 0.5 M NaCl, pH 7.3) containing 0.05% Triton × -100 and incubated with secondary biotin-labeled antibody (Multi Link, swine anti-immunoglobulins, Dako E0453, Denmark; 1:200v/v) for 2 h at room temperature. After three washes in TBS 1 and

TBS 2 (0.1 M Tris HCl, 0.1 M NaCl, pH 9.4), detection was performed with streptavidin alkaline phosphatase (ALP) (DAKO, Glostrup, Denmark) and reactivity visualized using the naphthol AS-MX phosphate/fast red TR salt capture method (Zreiqat et al. 1996).

Levamisole (5 mM) was added to inhibit endogenous ALP activity. Sections were counterstained with Harris's hematoxylin for 10 s and mounted directly with Crystal/Mount (Biomedica, Foster City, CA, USA).

Histochemistry

Alkaline phosphatase was detected at pH 9.2 using the naphthol phosphate method (Chayen and Bitensky 1981) with fast red violet LB base as coupler. Resin-embedded sections were stained in Von-Kossa solution (1% AgNO₃/H₂O) and incubated under UV light for 5–10 min before air-drying. Sections were mounted in Eukitt (Zeis, BRD).

Cell culture preparation

Bone marrow stromal stem cells (BMSSC) from human donors were prepared as previously described (Gronthos et al. 2003). Briefly, primary BMSSC cultures were established from STRO-1⁺ MACS-isolated bone marrow mononuclear cells in α -MEM supplemented with 20% fetal calf serum (FCS), 100 μ M L-ascorbate-2-phosphate, 2 mM L-glutamine, 50 U/ml penicillin and 50 μ g/ml streptomycin (JRH Biosciences, Lenexa, KS, USA). Cultured BMSSC (passages two and four) were used for flow cytometric analysis and Reverse transcriptase-polymerase chain reaction (RT-PCR).

Fluorescence-activated cell sorting (FACS)

Single cell suspensions were generated from secondary BMSSC cultures following trypsin/EDTA digestion. The cells were incubated with anti-STRO-1 (mouse IgM anti-human stromal stem cells (Gronthos et al. 2003) and ALP (B4-78, mouse IgG anti-human ALP; Developmental Studies Hybridoma Bank, University of Iowa, Iowa) or isotype control antibodies [1A6.12, (IgM) and 3D3 kindly provided by Prof. L. K. Ashman, University of Newcastle, Australia], for 60 min on ice (isotype matched antibodies, STRO-1 and B4-78 tissue culture supernatants were used at a dilution of 1:2). After washing, the cells were incubated with goat anti-mouse IgG conjugated with FITC and goat anti-mouse IgM conjugated with PE (1/50; Southern Biotechnology Associates, Birmingham, AL, USA) for an additional 30 min on ice. Cells were double sorted for purity using a FACStar^{PLUS} flow cytometer (Becton Dickinson, Sunnyvale, CA, USA) into four populations: STRO-1⁺/B478⁻, STRO-1⁺/B478⁺, STRO-1⁻/B478⁺ and

STRO-1⁻/B478⁻ as previously described (Gronthos et al. 1999, JBMR paper). For single color flow cytometric analysis, cells were first fixed with 1% paraformaldehyde then washed with 0.1% saponin solution before incubating with the rabbit anti-S100A8 IgG or control rabbit Ig (Caltag Laboratories, San Francisco, CA, USA) at 10 μ g/ml for 1 h at room temperature. After washing, cells were incubated with PE-conjugated goat anti-rabbit Ig for 30 min at RT. Cells were analyzed as described above.

Reverse transcriptase polymerase chain reaction (RT-PCR) analysis

Total cellular RNA was prepared from unsorted BMSSC, and from STRO-1⁺/B478⁺, STRO-1⁺/B478⁻, STRO-1⁻/B478⁺, STRO-1⁻/B478⁻, sorted cells using RNeasy extraction (Qiagen, Crawley, Australia), according to the manufacturer's recommendations. Total RNA from each population was used as a template for cDNA synthesis, prepared using a First-strand cDNA synthesis kit (Pharmacia Biotech, Uppsala, Sweden). The expression of various transcripts was assessed by PCR amplification, using a standard protocol as described previously (Gronthos et al. 2003). Primer sets:

S100A8 Fwd GGGATGACCTGAAGAAATTGCTA;
S100A8 Rev TGTTGATATCCAACCTCTTTGAACCA;
S100A9 Fwd GTGCGAAAAGATCTGCAAAATTT;
S100A9 Rev GGTCCTCCATGATGTGTTCTATGA;
 β -actin Fwd AGCCATGTACGTTGCTA;
 β actin Rev AGTCCGCCTAGAAGCA-3.

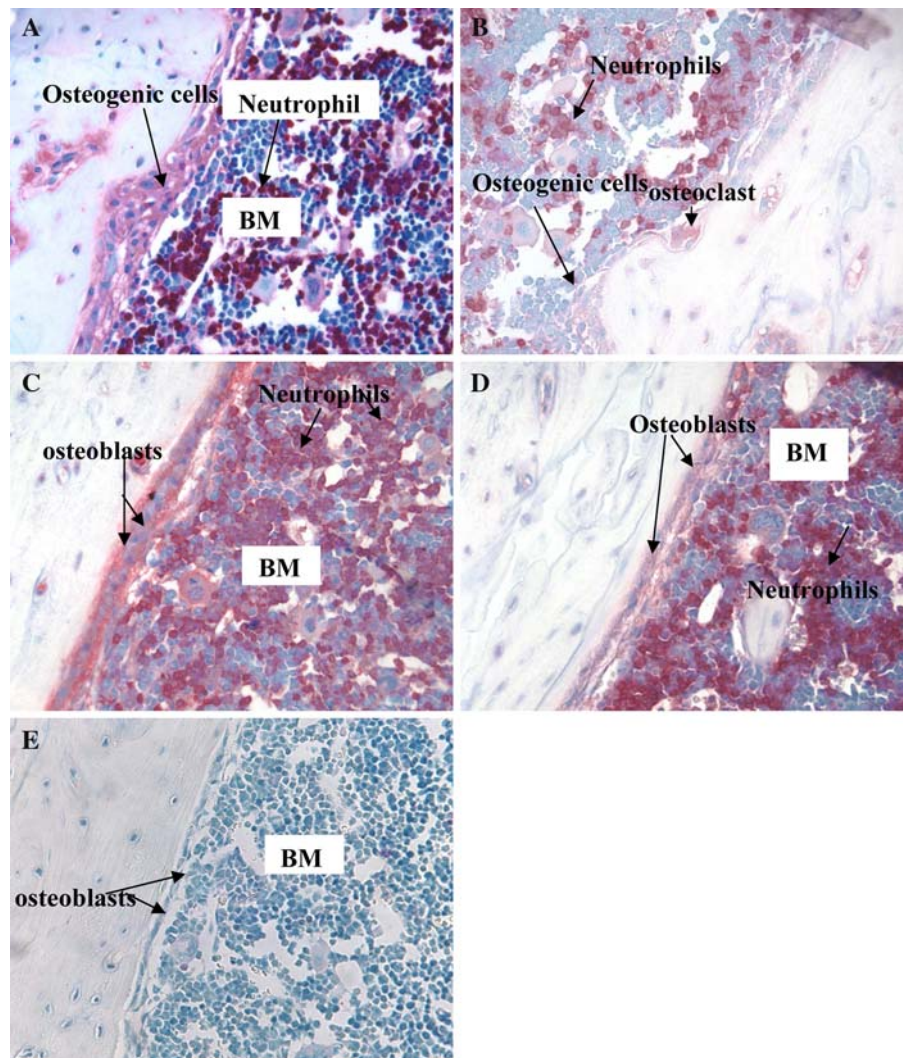
Following amplification, each reaction mixture was analyzed by 1.5% agarose gel electrophoresis, and visualized by ethidium bromide staining. RNA integrity was assessed by the expression of β -actin.

Results

A8 and A9 expression in murine osteoblasts and osteoclasts

The presence of A8 and A9 was first examined in tibias and femurs collected from 2, 4, and 8-week old mice. In addition to their expected strong immunoreactivity in neutrophils within the bone marrow of all tissues (Fig. 1), these proteins were differentially present in bone (Figs. 1, 3) and cartilage cells (Figs. 2, 3, 4). A8 was found in pre-osteoblasts (osteogenic cells) in the endosteal zone of femurs and tibias at 2 (results not shown), 4 (Fig. 1a) and 8 weeks (Fig. 1c). In marked contrast, no significant A9 reactivity was detected in any osteogenic cells in these areas at 2

Fig. 1 Sections from a 4 and 8 weeks old mouse stained with anti-A8 and anti-A9. Positive A8 reactivity was obvious in the osteogenic layer (A) whereas no anti-A9 (B) reactivity was seen. A8 (A) and A9-positive (B) neutrophils were present in the bone marrow (BM). Sections from mice at 8 weeks contained A8-positive (C) but A9-negative (D) osteoblasts. Neutrophils in the bone marrow were strongly positive for both proteins. Control sections from mice at 8 weeks (E), non-immune IgG produced no background staining. Positively-stained cells (red). Counterstained with haematoxylin, bright field microscopy; magnification 400x



(results not shown), 4 (Fig. 1b) or 8 (Fig. 1d) weeks. Non-immune IgG produced no background staining (Fig. 1e).

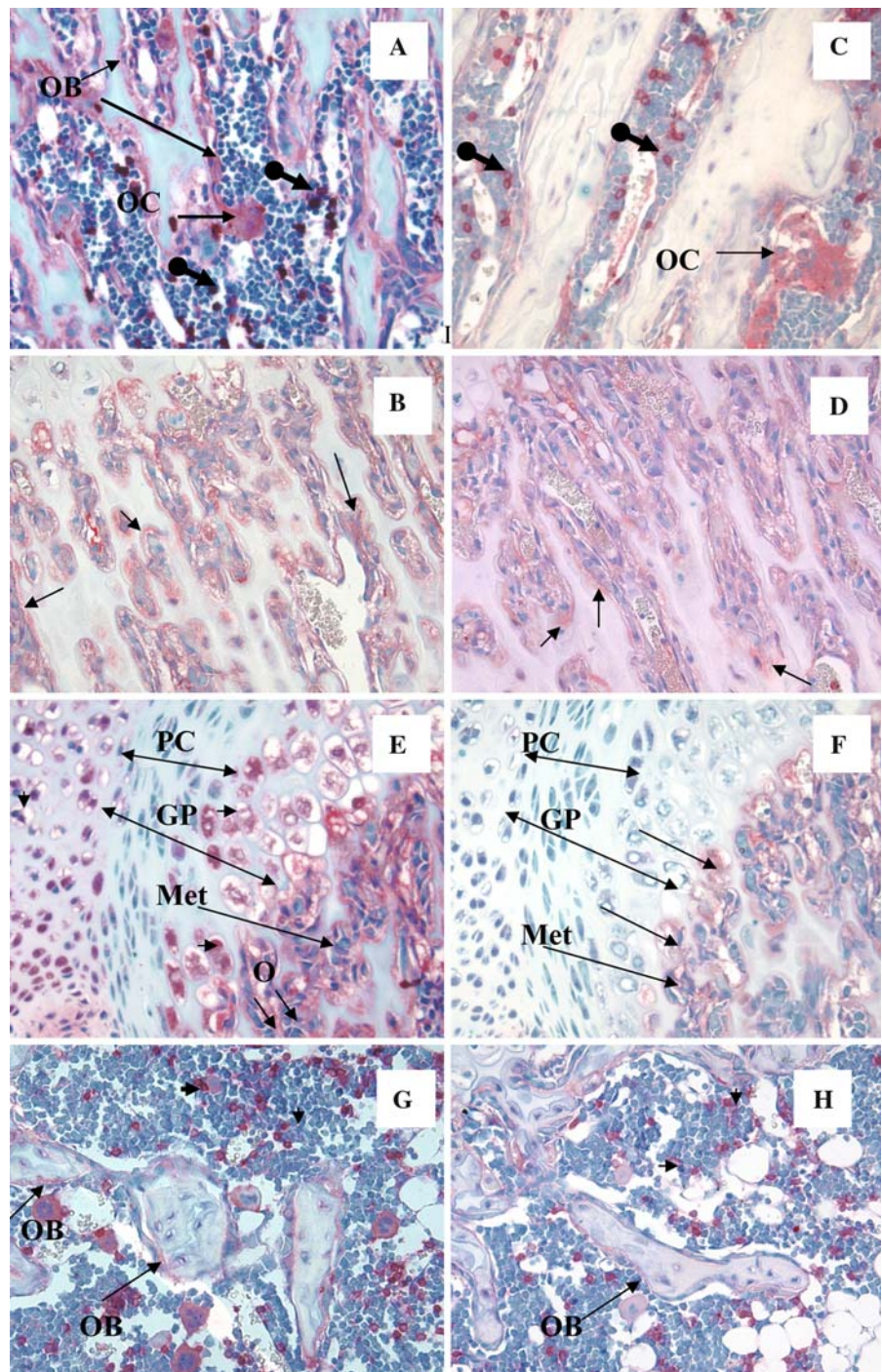
Osteoblasts in the central portion of the primary spongiosa in bone from mice at 2 (Fig. 2a {A8}), 4 (Fig. 2b {A8}) and 8 weeks (results not shown) stained strongly for A8 but weakly for A9 at 4 (Fig. 2d) and 8 weeks (results not shown). Immunoreactivity for A8 and A9 was also clearly evident within multinucleated osteoclasts at 2 (Fig. 2a {A8}), 4 (results not shown) and 8 (Fig. 2c {A9}) weeks. Strong A8 immunoreactivity occurred in osteoblasts and chondrocytes at the growth plate within the metaphyseal diaphyseal remodeling zone, particularly near the perichondrium. A representative figure from a 2-week old mouse is shown (Fig. 2e). In contrast, osteoblasts in these areas only stained weakly for A9 (Fig. 2f) and low reactivity of anti-A8 (Fig. 2g) and anti-A9 (Fig. 2h) was evident in the peripheral epiphyseal remodeling zones, as shown in the representative figure of bone harvested at 2 weeks.

The high levels of apparent A8 and A9 immunoreactivity in osteoclasts were consistent with mRNA expression data. We published a comparative affymetrix array profile of mouse primary calvarial osteoblasts, culture-derived osteoclasts and macrophages at <http://symatlas.gnf.org>. Under conditions where there was no detectable expression of A8 or A9 mRNA in macrophages or osteoblasts, osteoclast expression was at least 4 orders of magnitude above the detection threshold. In the same datasets, A8 and A9 mRNA expression in a wide range of mouse tissues is 4–5 orders of magnitude higher in bone than in spleen, which has a substantial myeloid cell population (data not shown).

Expression of A8 and A9 in human bone cells

Expression array profiling (symatlas.gnf.org) confirms high A8 and A9 mRNA expression in human bone, but the samples used would have included other cell populations

Fig. 2 Immunohistochemistry of sections from tibias from 2, 4, and 8 week old mice; A8 (A) was expressed in osteoclasts (OC) and osteoblasts (OB) from 2 week old mice. Neutrophils in bone marrow stained strongly for A8 (arrows with round ends). At 4 weeks (B), the primary spongiosa displaying cartilaginous matrix contained A8-positive osteoblasts (arrows). (C) shows metaphyseal bone containing A9-positive osteoclasts, but not osteoblasts in bone from an 8 week old mouse whereas the primary spongiosa from mice at 4 weeks (D) contained A9-positive osteoblasts (arrows). (E) The junction of the growth plate (GP)/metaphyseal (Met) remodeling zone from a 2 week old mouse is shown; PC: proliferating chondrocytes. Hypertrophic chondrocytes in the epiphysis and growth plate (small arrow heads) were highly A8-positive and osteogenic cells (O) strongly expressed A8. In contrast, hypertrophic chondrocytes in the epiphysis and growth plate (arrow heads) were A9-negative (F); osteogenic cells were strongly A9 positive. In the peripheral osteogenic region of the epiphysis of the distal femur and upper tibia from mice at 2 weeks, A8-positive (G) and weakly A9-positive osteoblasts (H) were obvious. A8 and A9-positive neutrophils (arrow heads) are indicated throughout. Positively-stained cells (red). Counterstained with haematoxylin, bright field microscopy; magnification 400x

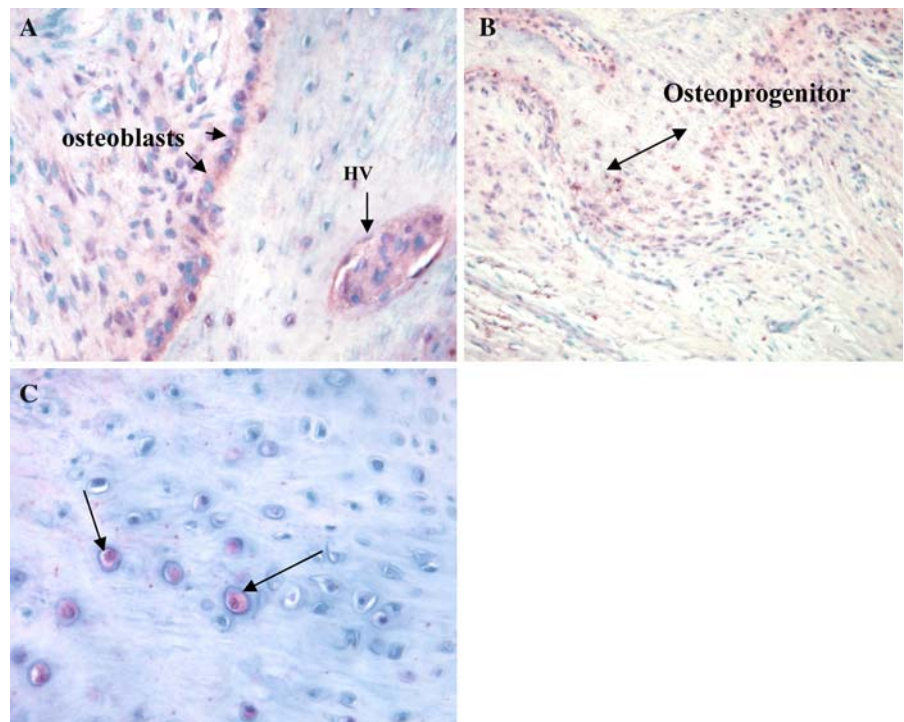


such as myeloid cells. To compare with expression patterns found in the mouse, and to confirm that A8 is expressed in human bone, we obtained samples from sites undergoing rapid remodeling. Figure 3a shows active remodeling adjacent to an aseptic loosened prosthesis, with A8-positive osteoblasts (Fig. 3a) and osteoprogenitor cells (Fig. 3b). A8 was seen in large hypertrophic chondrocytes (HC) within the calcaneal cartilage from a 2-year old boy (Fig. 3c) and in osteoclasts (results not shown).

Expression of A8 and A9 in human bone marrow stromal stem cells

To confirm expression indicated by staining of human cells and tissue, cultured human BMSSC were used. RT-PCR analysis detected A8 transcripts in these cells whereas no A9 mRNA was evident (Fig. 4a). Single-color flow cytometric analysis confirmed low levels of cytoplasmic A8 in these cells (Fig. 4b). Dual-color FACS was used to partition

Fig. 3 Periprosthetic tissue of adult human bone taken from patient with an aseptically loosened prosthesis harvested a few millimeters from the interfacial pathology where the bone appeared to be reactive. A8-positive osteoblasts were evident (A), within the Harvasian Canal (HV) and in osteoprogenitor cells (B). In femoral bone from a two year old boy (C), A8 expression was seen in large chondrocytes within the calcaneal cartilage, in which there were areas of degenerative hypertrophic chondrocytes (arrows). Positively-stained cells (red). Counterstained with haematoxylin, bright field microscopy; original magnification A and C, 400x; B, 200x



different BMSSC STRO-1/B4-78 subfractions. STRO-1 identifies stromal precursor cells and B4-78 reacts with the osteoblast associated marker, ALP, as shown in Fig. 4c, represented in regions R1-R4 (Gronthos et al. 1999; Stewart et al. 1999). The different STRO-1/B4-78 BMSSC subpopulations demonstrated a heterogeneous but highly reproducible pattern of A8 expression detected using semiquantitative RT-PCR (Fig. 4d). The most immature pre-osteogenic stromal population STRO-1⁺/B4-78 (R1, osteoprogenitors) expressed high levels of A8 in contrast to the lower amounts in the more committed pre-osteoblastic cell fraction (R2, STRO-1⁺/B4-78⁺). Furthermore, a larger proportion of the stromal population consisting of the most mature cell populations STRO-1⁻/B4-78⁺ (R4, osteoblasts) and STRO-1⁻/B4-78⁻ (R3, osteocytes and bone lining cells) had lower detectable A8 mRNA levels (Fig. 4c, d).

Hypertrophic chondrocytes express A8 and A9

Chondrocytes of the resting and proliferating zones of growth plates did not express A8 or A9 in bones from 2, 4 or 8-week old mice. In contrast, A8 immunoreactivity was detected throughout the zones of maturing and degenerating HC of the growth plate as shown in the representative figure from a 2-week old mouse (Fig. 5a, b). A9 was only evident in the invading vascular-osteogenic tissue penetrating the degenerating chondrocytic zone adjacent to the primary spongiosa (Fig. 5d).

Association of A8 and A9 with sites of calcification

Sections from undecalcified bone from 2, 4, and 8-week old mice were processed by embedding in hydroxyl ethyl methacrylate (HEMA). These showed similar positive patterns of A8 expression (shown in the representative figure of bone harvested from 2-week old mice; Fig. 6a), although reactivity in HC was less intense than that seen in paraffin sections (see Fig. 5). The calcified cartilaginous matrix of the HC and articular cartilage zones stained strongly for A8 (arrow) where cellular ALP activity (Fig. 6c) and matrix calcification were apparent (Fig. 6b, e). The immunoreactivity pattern of A9 in this area was not different. The central zone of the epiphysis is replaced by bone in a process referred to as secondary osteogenesis. A9 was detected in the in-growing vascular penetration from the zone of osteogenesis (not shown). HC and their interterritorial matrix of the proximal tibial epiphysis from 2-week old mice, expressed A8 (arrows) (Fig. 6d). Positive Von Kossa staining (arrow) confirmed calcification in the HC zone (Fig. 6e).

Discussion

In this study, A8 and A9 were both detected in bone and cartilage cells, but their precise location, and hence their inferred function, was discordant. Only A8 was seen in

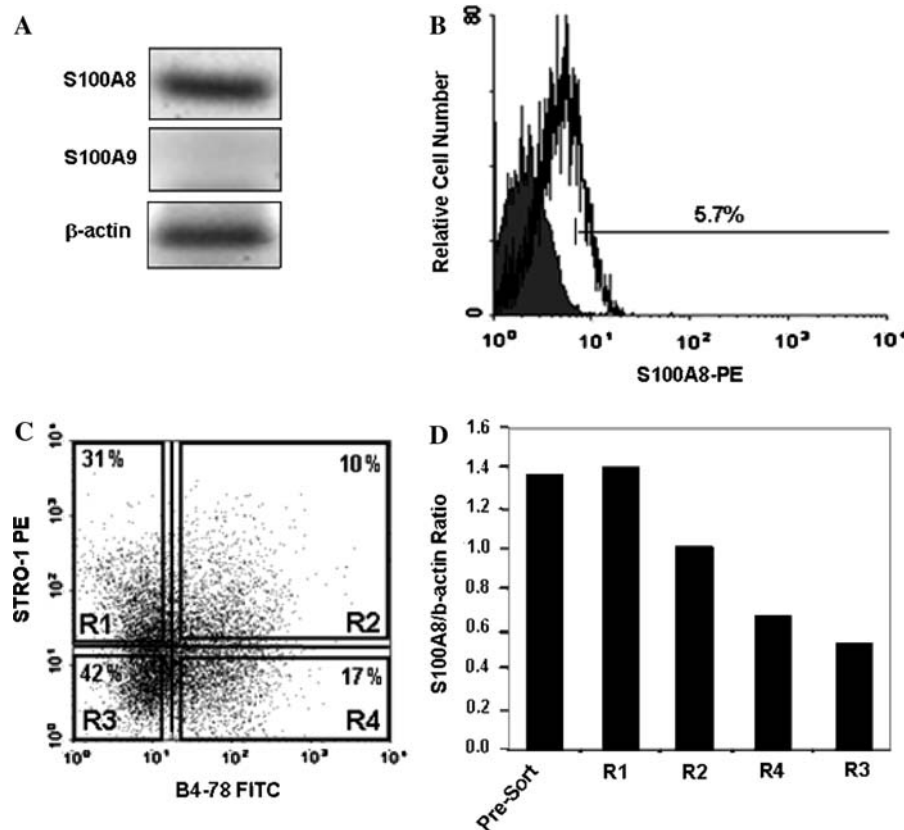


Fig. 4 Expression of S100A8 by bone marrow stromal stem cells (BMSSC). (A) RT-PCR analysis for S100A8, S100A9 and beta-actin transcripts in cultured BMSSC. (B) Singlecolour flow cytometric analysis demonstrating low cytoplasmic expression of S100A8 by human cultured BMSSC (open histogram) and isotype control antibody (shaded histogram). (C) Dual-colour FACS was employed to isolate different BMSSC subfractions following separation based on their expression of the stromal precursor cell marker STRO-1 and the osteoblastic marker ALP (B4-78) according to regions R1- R4.

preosteogenic cells whereas osteoblasts had variable, but generally weak expression of both proteins. Only A8 was detected in the BMSSC population. BMSSC subpopulations exhibited a heterogeneous but highly reproducible pattern of A8 mRNA expression *in vitro* while no A9 expression was found. The data showed that immature preosteogenic stromal cells expressed high levels of A8 that decreased in the more committed pre-osteoblastic cells, suggesting that A9 maybe switched on only at the differentiation stage. Therefore, the observed differential expression of A8 and the lack of A9 expression in these stromal subpopulations suggest a possible role for A8 during osteoblast differentiation.

Hypertrophic chondrocytes and primary ossification centers

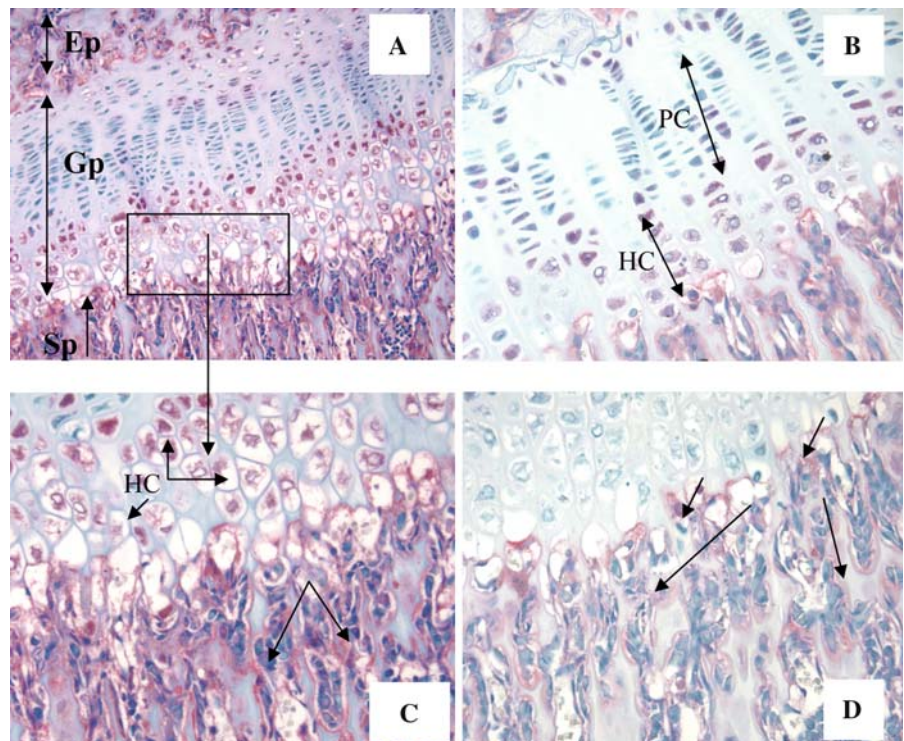
In the femurs and tibias from 2, 4, and 8-week old mice, within this developmental pathway A8, but not A9, was

(D) The different STRO-1/ALP BMSSC subpopulations demonstrated a heterogeneous but highly reproducible pattern of A8 expression using semiquantitative RT-PCR analysis. The most immature preosteogenic stromal population (R1) expressed high levels of A8 in contrast to the more committed preosteoblastic cell fraction (R2). A larger proportion of the stromal population consisting of mature osteoblasts (R4), osteocytes and bone lining cells (R3) had lower detectable levels of A8 mRNA

expressed in the HC zones of the growth plates, but not in their proliferating zones. Both proteins were expressed in the extracellular cartilage matrix, only within calcifying areas (as indicated by von Kossa staining and ALP-positive cells) of the epiphyseal cartilage. A9 has strong affinity for heparin and binds A8, thus allowing their localization within the matrix (Harrison et al. 1999) and, together with the presence of A9 in calcifying microvesicles isolated from calcifying atherosclerotic lesions (McCormick et al. 2005), we propose that these proteins are involved in regulation of calcification that occurs in the HC zone and its replacement with trabecular bone matrix. Most terminally differentiated chondrocytes in the fetal growth plate undergo apoptotic cell death and changes in the cartilage matrix of the hypertrophic zone allow invasion by capillaries, degradation of the calcified cartilage matrix and its replacement with trabecular bone matrix secreted by invading osteoblasts.

There is significant differential gene expression between proliferating and HC (Wang et al. 2004). For example,

Fig. 5 Immunohistochemistry of sections from the proximal end of the tibia from a 2 week old mouse (A) including epiphysis (Ep), growth plate (Gp) and spongiosa (Sp). (B) Positive reactivity with anti-A9 was obvious in the invading osteogenic cells of the primary spongiosa (arrows) and the hypertrophic chondrocytes (HC); proliferating chondrocytes (PC) did not stain with anti-A9. (C) Strong staining was found with anti-A8 in the hypertrophic chondrocyte (HC) and osteoblasts (arrows) at the junction of the growth plate and spongiosa (high power of Fig 4A). (D) The junction of the growth plate and spongiosa contained A9-positive osteoblasts (arrows). Counterstained with haematoxylin, bright field microscopy, original magnification is A, 200x; B, C and D 400x



immature (proliferating) chondrocytes secrete angiogenic inhibitors (Alini et al. 1996; Engsig et al. 2000), whereas HC produce factors (Moses et al. 1999; Shukunami et al. 1999) that could promote angiogenesis (Alini et al. 1996; Engsig et al. 2000). A8 and A9 were both evident in isolated regions at junctions of the growth plate cartilage and the primary spongiosa. In particular, A9 was confined to preosteogenic invading vascular sprouts and both proteins were prominently colocalized in regions of intense vascular remodeling, where A8 was also present. At the cartilage-bone interface, only a thin layer of cartilage matrix separates HC from invading capillaries. This layer, known as the last transverse septa (Lee et al. 1996), actively undergoes matrix remodeling and trabecular bone is laid down on remnants of calcified cartilage (Stickens et al. 2004). In these isolated regions, invading vascularized mesenchymal tissue is preceded by chondroclasts. It is difficult at a light microscopic level to ascertain whether only vascularized mesenchymal cells, or portions of chondroclasts are present. The dual localization of A8 and A9 in the zone at the last transverse septum suggests their co-expression in a particular cell type referred to as “septoclasts” (Lee et al. 1995) in this area.

A8 and A9 are expressed by activated microvascular endothelial cells in vitro (Yen et al. 1997) and in microvessels in areas of inflammatory neovascularization (McCormick et al. 2005). The A8/A9 complex can bind the endothelium and up-regulates a number of pro-inflammatory genes and adhesion receptors and influences expres-

sion of surface receptors involved in endothelial growth and differentiation and monolayer integrity (Viemann et al. 2004), processes important in vascular neogenesis.

The role of A8 and A9 in osteoclasts: an observation

Immunohistochemistry of murine and human bone sections confirmed published mRNA data (<http://symatlas.gnf.org>) indicating very high A8 and A9 expression in osteoclasts. Given the chemotactic activity of A8, and its essential role in implantation, it is possible that it acts as a signaling molecule coupling osteoclast and osteoblast activity to provide calcium homeostasis, or to provide a matrix for recalcification following resorption. One or both proteins could also participate directly in regulating bone resorption. Given these observations, the apparent immunoreactivity of osteoblasts must be considered with some caution, since they may have bound S100 protein derived from osteoclasts or other cells associated with bone surfaces.

Some processes important in bone remodeling are regulated by reactive oxygen intermediates (ROI). For example, low concentrations of H_2O_2 or O_2^- accelerate resorption by osteoclasts and HOCl and hydroxyl radicals can degrade proteoglycans and fragment collagen. HOCl can also alter matrix metalloproteinase (MMP) activity by inactivating tissue inhibitors of MMP and activating certain MMPs (reviewed in Hadjigogos 2003). Moreover, oxidants stimulate osteoclastic differentiation and anti-oxidant

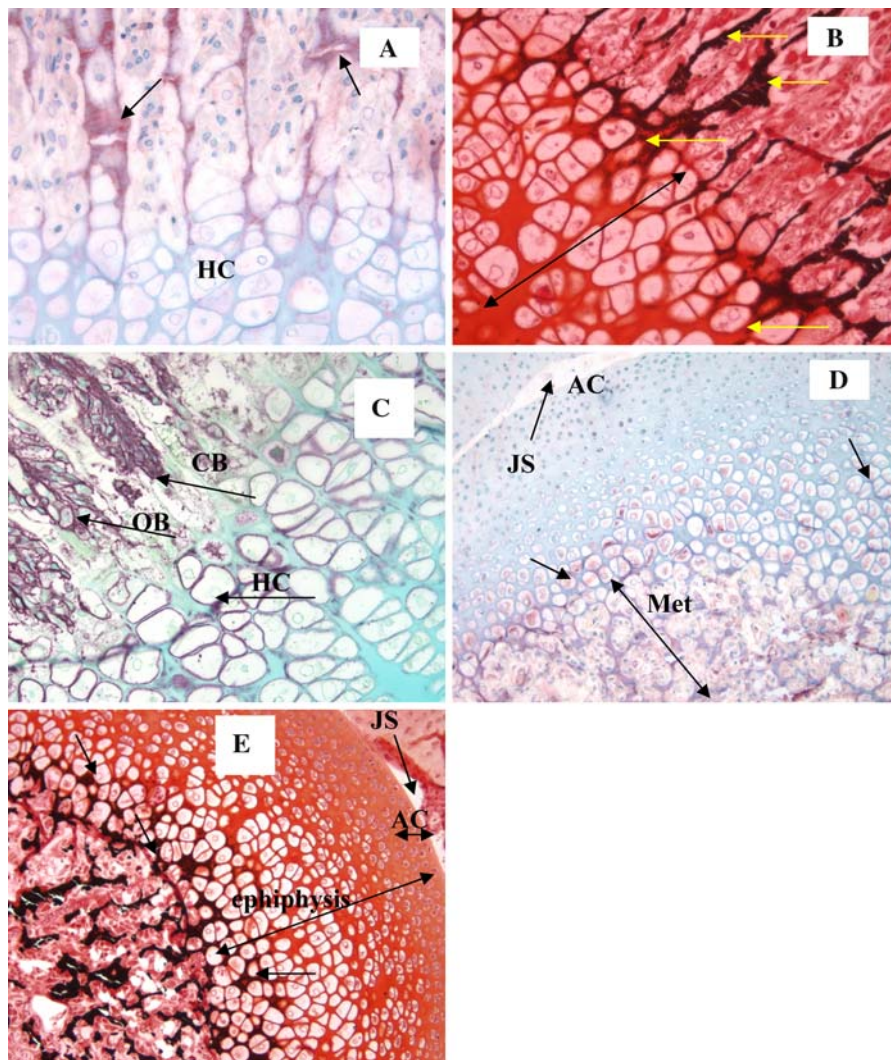


Fig. 6 Expression of A8 (A, D) alkaline phosphates (C) and staining for Von Kossa (B, E) in the hypertrophic chondrocyte zone of the growth plate from the upper tibia of 2 a week old mouse. Although the hypertrophic chondrocytes (HC) only reacted weakly with anti-A8, compared to the paraffin section (see Fig 4), (A) the calcified cartilaginous matrix was strongly A8 positive (arrow). (B) Positive Von Kossa staining in the calcified matrix of bone and cartilage at the junction of the growth plate and primary spongiosa is indicated (arrows). No calcification was evident in the primary spongiosa (double arrow). (C) Alkaline phosphatase, assessed by enzyme

histochemistry was obvious in hypertrophic chondrocytes (HC, arrows), early calcified bone (CB, arrows) and osteoblasts (OB, arrows). (D) Joint space (JS), the articular cartilage (AC), epiphysis and the metaphysis (MET) from the proximal end of the tibia where hypertrophic chondrocytes expressed A8 (arrows). (E) Von Kossa stain (arrow) indicates areas of calcification in the hypertrophic chondrocytic zone. Tissue embedded in hydroxy ethyl methacrylate. Immunohistochemistry staining, Positive stained cells (red), Counterstained with methylene green, bright field microscopy, magnification, 400x

proteins regulate this process and H_2O_2 inhibits osteoblast differentiation in BMSSC which can be negated by induction of the anti-oxidant protein, metallothionein (Liu et al. 2004). Some S100 proteins can regulate oxidative processes. An important function of A8, and possibly A9, is their ability to scavenge oxidants such as H_2O_2 and HOCl (Harrison et al. 1999; Raftery et al. 2001) and a protective function for these proteins in acute inflammation and in atherogenesis (Rahimi et al. 2005) is proposed. Thus, A8 and/or A9 may contribute to regulation of the oxidative balance necessary for bone remodeling.

Conclusion

The observational data from mice, human provide evidence that A8 and A9 may be involved in processes of osteoblast and chondrocytic maturation and matrix calcification. Furthermore these proteins may also play a role in flord osteogenesis in the primary spongiosa. These data provide the rationale for more detailed studies of the bone phenotype and calcium turnover in A9-null animals, and possible generation of a bone-specific A8 knockout to discern their true functions.

Acknowledgments The authors would like to acknowledge the Australia National Health and Medical Research Council and the Australian Research Council. We thank Mrs. Barbara James for preparing all the bone sections and histological staining. We thank Associate Professors Christopher Little and Brian Freeman for their editorial assistance and valuable comments during the preparation of this manuscript. We thank Professor Boskey and colleagues for their discussion on nucleation studies.

References

- Alini M, Marriott A, Chen T, Abe S, Poole AR (1996) A novel angiogenic molecule produced at the time of chondrocyte hypertrophy during endochondral bone formation. *Dev Biol* 176:124–132
- Al-Rasheed A, Scheerens H, Rennick DM, Fletcher HM, Tatakis DN (2003) Accelerated alveolar bone loss in mice lacking interleukin-10. *J Dent Res* 82:632–635
- Balmain N, Moutahir F, Heizmann CW, Lieberherr M (2003) Immunolocalization of S100A2 calcium-binding protein in cartilage and bone cells. *Cell Mol Biol (Noisy-le-grand)* 49:485–486
- Chayen J, Bitensky L (1981) Cytochemistry in the bioassay of hormones. *J Clin Pathol* 34:575–588
- Cornish CJ, Devery JM, Poronnik P, Lackmann M, Cook DI, Geczy CL (1996) S100 protein CP-10 stimulates myeloid cell chemotaxis without activation. *J Cell Physiol* 166:427–437
- Donato R (2001) S100: a multigenic family of calcium-modulated proteins of the EF-hand type with intracellular and extracellular functional roles. *Int J Biochem Cell Biol* 33:637–668
- Duarte WR, Shibata T, Takenaga K, Takahashi E, Kubota K, Ohya K, Ishikawa I, Yamauchi M, Kasugai S (2003) S100A4: a novel negative regulator of mineralization and osteoblast differentiation. *J Bone Miner Res* 18:493–501
- Engelkamp D, Schafer BW, Mattei MG, Erne P, Heizmann CW (1993) Six S100 genes are clustered on human chromosome 1q21: identification of two genes coding for the two previously unreported calcium-binding proteins S100D and S100E. *Proc Natl Acad Sci U S A* 90:6547–6551
- Engsig MT, Chen QJ, Vu TH, Pedersen AC, Therkidsen B, Lund LR, Henriksen K, Lenhard T, Foged NT, Werb Z, Delaisse JM (2000) Matrix metalloproteinase 9 and vascular endothelial growth factor are essential for osteoclast recruitment into developing long bones. *J Cell Biol* 151:879–889
- Foell D, Hernandez-Rodriguez J, Sanchez M, Vogl T, Cid MC, Roth J (2004) Early recruitment of phagocytes contributes to the vascular inflammation of giant cell arteritis. *J Pathol* 204:311–316
- Gronthos S, Zannettino AC, Graves SE, Ohta S, Hay SJ, Simmons PJ (1999) Differential cell surface expression of the STRO-1 and alkaline phosphatase antigens on discrete developmental stages in primary cultures of human bone cells. *J Bone Miner Res* 14(1):47–56
- Gronthos S, Zannettino AC, Hay SJ, Shi S, Graves SE, Kortessidis A, Simmons PJ (2003) Molecular and cellular characterisation of highly purified stromal stem cells derived from human bone marrow. *J Cell Sci* 116:1827–1835
- Hadjigogos K (2003) The role of free radicals in the pathogenesis of rheumatoid arthritis. *Panminerva Med* 45:7–13
- Harrison CA, Raftery MJ, Walsh J, Alewood P, Iismaa SE, Thliveris S, Geczy CL (1999) Oxidation regulates the inflammatory properties of the murine S100 protein S100A8. *J Biol Chem* 274:8561–8569
- Helfman DM, Kim EJ, Lukanidin E, Grigorian M (2005) The metastasis associated protein S100A4: role in tumour progression and metastasis. *Br J Cancer* 92:1955–1958
- Hobbs JA, May R, Tanousis K, McNeill E, Mathies M, Gebhardt C, Henderson R, Robinson MJ, Hogg N (2003) Myeloid cell function in MRP-14 (S100A9) null mice. *Mol Cell Biol* 23:2564–2576
- Hofmann MA, Drury S, Fu C, Qu W, Taguchi A, Lu Y, Avila C, Kambham N, Bierhaus A, Nawroth P, Neurath MF, Slattery T, Beach D, McClary J, Nagashima M, Morser J, Stern D, Schmidt AM (1999) RAGE mediates a novel proinflammatory axis: a central cell surface receptor for S100/calgranulin polypeptides. *Cell* 97:889–901
- Iismaa SE, Hu S, Kocher M, Lackmann M, Harrison CA, Thliveris S, Geczy CL (1994) Recombinant and cellular expression of the murine chemotactic protein, CP-10. *DNA Cell Biol* 13:183–192
- Kerkhoff C, Nacken W, Benedyk M, Dagher MC, Sopalla C, Doussiere J (2005) The arachidonic acid-binding protein S100A8/A9 promotes NADPH oxidase activation by interaction with p67phox and Rac-2. *Faseb J* 19:467–469
- Laboux O, Ste-Marie LG, Glorieux FH, Nanci A (2003) Quantitative immunogold labeling of bone sialoprotein and osteopontin in methylmethacrylate-embedded rat bone. *J Histochem Cytochem* 51(1):61–67
- Lee ER, Lamplugh L, Shepard NL, Mort JS (1995) The septoclast, a cathepsin B-rich cell involved in the resorption of growth plate cartilage. *J Histochem Cytochem* 43:525–536
- Lee K, Lanske B, Karaplis AC, Deeds JD, Kohno H, Nissenson RA, Kronenberg HM, Segre GV (1996) Parathyroid hormone-related peptide delays terminal differentiation of chondrocytes during endochondral bone development. *Endocrinology* 137:5109–5118
- Liu AL, Zhang ZM, Zhu BF, Liao ZH, Liu Z (2004) Metallothionein protects bone marrow stromal cells against hydrogen peroxide-induced inhibition of osteoblastic differentiation. *Cell Biol Int* 28:905–911
- Makino E, Sakaguchi M, Iwatsuki K, Huh NH (2004) Introduction of an N-terminal peptide of S100C/A11 into human cells induces apoptotic cell death. *J Mol Med* 82:612–620
- Manitz MP, Horst B, Seeliger S, Strey A, Skryabin BV, Gunzer M, Frings W, Schonlau F, Roth J, Sorg C, Nacken W (2003) Loss of S100A9 (MRP14) results in reduced interleukin-8-induced CD11b surface expression, a polarized microfilament system, and diminished responsiveness to chemoattractants in vitro. *Mol Cell Biol* 23:1034–1043
- McCormick MM, Rahimi F, Bobryshev YV, Gaus K, Zreiqat H, Cai H, Lord RS, Geczy CL (2005) S100A8 and S100A9 in human arterial wall: Implications for atherogenesis. *J Biol Chem* 280(50):41521–41529
- McNutt NS (1998) The S100 family of multipurpose calcium-binding proteins. *J Cutan Pathol* 25:521–529
- Moses MA, Wiederschain D, Wu I, Fernandez CA, Ghazizadeh V, Lane WS, Flynn E, Sytkowski A, Tao T, Langer R (1999) Troponin I is present in human cartilage and inhibits angiogenesis. *Proc Natl Acad Sci U S A* 96:2645–2650
- Passey RJ, Williams E, Lichanska AM, Wells C, Hu S, Geczy CL, Little MH, Hume DA (1999b) A null mutation in the inflammation-associated S100 protein S100A8 causes early resorption of the mouse embryo. *J Immunol* 163:2209–2216
- Passey RJ, Xu K, Hume DA, Geczy CL (1999a) S100A8: emerging functions and regulation. *J Leukoc Biol* 66:549–556
- Raftery MJ, Yang Z, Valenzuela SM, Geczy CL (2001) Novel intra- and inter-molecular sulfonamide bonds in S100A8 produced by hypochlorite oxidation. *J Biol Chem* 276:33393–33401
- Rahimi F, Hsu K, Endoh Y, Geczy CL (2005) FGF-2, IL-1beta and TGF-beta regulate fibroblast expression of S100A8. *Febs J* 272:2811–2827
- Ravasi T, Hsu K, Goyette J, Schroder K, Yang Z, Rahimi F, Miranda LP, Alewood PF, Hume DA, Geczy C (2004) Probing the

- S100 protein family through genomic and functional analysis. *Genomics* 84:10–22
- Roth J, Vogl T, Sorg C, Sunderkotter C (2003) Phagocyte-specific S100 proteins: a novel group of proinflammatory molecules. *Trends Immunol* 24:155–158
- Shukunami C, Iyama K, Inoue H, Hiraki Y (1999) Spatiotemporal pattern of the mouse chondromodulin-I gene expression and its regulatory role in vascular invasion into cartilage during endochondral bone formation. *Int J Dev Biol* 43:39–49
- Sorci G, Riuzzi F, Agneletti AL, Marchetti C, Donato R (2003) S100B inhibits myogenic differentiation and myotube formation in a RAGE-independent manner. *Mol Cell Biol* 23:4870–4881
- Sorci G, Riuzzi F, Agneletti AL, Marchetti C, Donato R (2004) S100B causes apoptosis in a myoblast cell line in a RAGE-independent manner. *J Cell Physiol* 199:274–283
- Stewart K, Walsh S, Screen J, Jefferiss CM, Chainey J, Jordan GR, Beresford JN (1999) Further characterization of cells expressing STRO-1 in cultures of adult human bone marrow stromal cells. *J Bone Miner Res* 14(8):1345–1356
- Stickens D, Behonick DJ, Ortega N, Heyer B, Hartenstein B, Yu Y, Fosang AJ, Schorpp-Kistner M, Angel P, Werb Z (2004) Altered endochondral bone development in matrix metalloproteinase 13-deficient mice. *Development* 131:5883–5895
- Viemann D, Goebeler M, Schmid S, Klimmek K, Sorg C, Ludwig S, Roth J (2004) Transcriptional profiling of IKK2/NF-kappa B- and p38 MAP kinase-dependent gene expression in TNF-alpha-stimulated primary human endothelial cells. *Blood* 103:3365–3373
- Vogl T, Ludwig S, Goebeler M, Strey A, Thorey IS, Reichelt R, Foell D, Gerke V, Manitz MP, Nacken W, Werner S, Sorg C, Roth J (2004) MRP8 and MRP14 control microtubule reorganization during transendothelial migration of phagocytes. *Blood* 104:4260–4268
- Wang Y, Middleton F, Horton JA, Reichel L, Farnum CE, Damron TA (2004) Microarray analysis of proliferative and hypertrophic growth plate zones identifies differentiation markers and signal pathways. *Bone* 35:1273–1293
- Yang Z, Tao T, Raftery MJ, Youssef P, Di Girolamo N, Geczy CL (2001) Proinflammatory properties of the human S100 protein S100A12. *J Leukoc Biol* 69:986–994
- Yen T, Harrison CA, Devery JM, Leong S, Iismaa SE, Yoshimura T, Geczy CL (1997) Induction of the S100 chemotactic protein, CP-10, in murine microvascular endothelial cells by proinflammatory stimuli. *Blood* 90:4812–4821
- Zreiqat H, Markovic B, Walsh WR, Howlett CR (1996) A novel technique for quantitative detection of mRNA expression in human bone derived cells cultured on biomaterials. *J Biomed Mater Res* 33:217–223